Tracer Dispersion in Sintered Glass Beads with a Bidisperse Size Distribution

An experimental study was made of tracer dispersion in bidisperse sintered glass materials prepared from mixtures of two sizes of beads with mean diameters of 325 and 95 μm. The equivalent dispersion coefficient increases by a factor of 30 when the porosity decreases from 30 to 12%; this variation is similar to that measured in monodisperse samples. The variation of dispersion can be characterized by the ratio $R = \ell_d / L_1$ where ℓ_d is a length scale deduced from the equivalent dispersion coefficient and L_1 is obtained from conductivity and permeability measurements. It is shown that the increase of ℓ_d / L_1 correlates with the loss of porosity during the sintering process. Lightly sintered samples with a percentage of small beads around the minimum of porosity display a nearly Gaussian behavior, with a dispersion coefficient close to that obtained in homogeneous equivalent mixtures. This result is in contrast with very large anomalies observed by other authors. These results imply that dispersion in consolidated samples is sensitive to large-scale inhomogeneities of the materials rather than to their detailed structure.

J. P. Hulin, E. Charlaix, T. J. Plona,
L. Oger, E. Guyon
Schlumberger Doll Research
Ridgefield, CT 06877

Introduction

The purpose of this paper is to study the influence on tracer dispersion of the polydispersity of the grains building up the solid matrix of a porous material. Tracer dispersion is presently of great interest both for its applications and for fundamental reasons. On the practical side, tracer dispersion can be used as a tool to detect structural inhomogeneities of rocks in hydrogeology or petroleum engineering. Dispersion is also useful in separating chemical components by their different adsorption characteristics in chromatography and chemical engineering processes. On a more fundamental level, tracer dispersion can be pictured as a biased random walk of tracer particles in a disordered system. This is a problem where recent statistical approaches of the physics of macroscopic disordered media have brought new physical insight.

For a homogeneous porous material fully saturated with a single liquid or a finely dispersed mixture, tracer dispersion can often be described by a convection-diffusion equation (Fried and Combarnous, 1971; Bear, 1972:

$$\frac{\partial C(x,t)}{\partial t} + (U \cdot \nabla)\, C(x,t) = K_{\parallel} \frac{\partial^2 C(x,t)}{\partial x_{\parallel}^2} + K_{\perp} \Delta_{\perp} C(x,t) \quad (1)$$

where U is the mean intersticial flow velocity. In Eq. 1, the two effective dispersion coefficients $K_{\parallel}$ and $K_{\perp}$ correspond to gradients of the tracer concentration either parallel or perpendicular to the flow. They take into account the effect of the random structure of the velocity field inside the medium. Solutions to Eq. 1 represent normal Gaussian dispersion; it is only valid when the upper boundary of the heterogeneity characteristic length scales is small compared to the sample size (in statistical language this condition is related to the application of the central limit theorem).

At high enough velocities, $K_{\parallel}$ is mainly associated with a geometrical mechanism (variation of the velocity field from one pore to another) with the approximate variation (Saffman, 1959, 1960):

$$K_{\parallel} \simeq U \ell_d \quad (2)$$

The length scale ℓ_d, often called dispersivity, is the basic information given by dispersion. The quantity ℓ_d can also be

---

The permanent address of J. P. Hulin, E. Charlaix, and E. Guyon is ESPCI, Laboratoire d'Hydrodynamique et de Mécanique Physique de l'ESPCI, unité associée au CNRS N°857, 10 rue Vauquelin, 75231 Paris, Cedex 05 France.

The permanent address of L. Oger is CERILH, 23 rue de Cronstadt, 75015 Paris, France.

described as the correlation length of the velocity-velocity correlation function (Bear, 1972; Koch and Brady, 1985, 1987) and thus as the mean characteristic length for the decorrelation of the velocity of a tracer particle along its path through the material. Note that the linear variation of $K_\parallel$ with U given in Eq. 2 is an approximation and other mechanisms introduce additional terms (Bear, 1972; Taylor, 1953, 1954; Koch and Brady, 1985, 1987; Guyon et al., 1987b).

Tracer dispersion and in particular ℓ_d can be a useful method to characterize the degree of heterogeneity of a porous medium. In a very homogeneous material, for example, the correlation length of the velocity field is very small and of the order of the grain size. On the contrary, correlation lengths much larger than the grain size are measured in many consolidated materials as well as real rocks (Baker, 1975; Coats and Smith, 1964; Bacri et al., 1986, 1987; Hulin and Salin, 1987. For instance, the dispersion coefficient in 200 μm dia. monodisperse glass beads samples (Charlaix et al., 1986, 1987) is almost two orders of magnitude higher in sintered beads with a porosity $\varnothing = 24\%$ than in nonconsolidated samples ($\varnothing = 37\%$). In addition, heterogeneous materials often demonstrate non-Gaussian dispersion curves (i.e., not solutions of Eq. 1 and hence described an anomalous) with characteristic long tails at large times (Baker, 1975; Charlaix et al., 1986, 1987; Coats and Smith, 1964; Lemaitre et al., 1986). Causes of heterogeneity can be many: at the pore scale, they may be due to a broad distribution of pore sizes (Charlaix et al., 1987; on a larger scale, they may be associated with random domains of higher and lower porosity.

The main objective of this work is to determine the relative influence of pore scale disorder as well as of longer range heterogeneities by studying dispersion in bidisperse packings of spherical beads as a function of their composition and of the degree of sintering. In addition, we will relate our results to recent experiments in unconsolidated mixtures of beads with binary size distributions (Lemaitre, 1985; Lemaitre et al., 1986; Guennelon et al., 1983) and double-peaked distributions (Han et al., 1985). The first three papers report very large effective dispersion coefficients in unconsolidated binary mixtures around the minimum of porosity (corresponding to a volume fraction of small spheres around 25%) (Ben Aim and Legoff, 1967; Ben Aim, 1970). The interpretation was related to the broad distribution of local currents due to the large pore size variations. Han et al., also measured larger dispersion coefficients (but only by a factor of 2) in binary mixtures than in monodisperse mixtures (however, in their experiment, the width of the peaks in the size distribution was larger and the fraction of large beads much smaller than reported here). These results imply an unexpectedly strong connection between the details of the microscopic structure and long-range correlations. This has induced us to study particularly closely the variations of the dispersion characteristics near the critical filling concentration.

Experimental Procedure

The experimental procedure has been described elsewhere (Charlaix et al., 1986, 1987). Either of two different $CaCl_2$-water solutions (1g/L and 2g/L) can be injected into the sample at a constant flow rate value. The time variation of concentration at the outlet of the sample is recorded after a stepwise variation has been induced at the inlet by switching from one solution to the other. The samples have a 12.5 mm OD and a length ranging between 5 and 15 cm. They are cored out of larger blocks of 10 cm dia.

The samples are prepared from beads with two different diameters, as was done by Lemaitre (1985) and Lemaitre et al. (1986). We have used beads in the two diameter ranges 88–104 and 297–354 μm. Several mixture compositions have been used. In particular, several samples of different compaction but with similar small bead volume fractions close to the critical value 30% have been analyzed. Great care has been taken to obtain homogeneous mixtures and to eliminate wall effects in the samples we have studied. Data on the fraction of small beads used in the bidipersed samples are contained in Table 1. The bidisperse samples will be labeled throughout the paper by their porosity.

The sample preparation procedure is the same as described elsewhere by Guyon et al. (1987a). The two types of beads are fed separately from vibrating distributors; the flow rates of each distributor can be adjusted to change the mixture composition. In order to obtain homogeneous concentrations of large and small spheres throughout the sample, the small particle feeder is periodically moved horizontally at a slow rate to improve their repartition. The feeders are placed above a cylindrical mold (10 cm ID, 20 cm height) which is continuously rotated in order to avoid stratification. The homogeneity of the packing is further improved by putting a series of screens between the feeders and the mold. After the mold is filled, it is placed inside a press and undergoes a series of pressure cycles to further eliminate inhomogeneities (Gauthier, 1987). Finally, the packing is consolidated by placing the cell in an oven at a temperature of 650°C for a length of time that depends on the required final porosity.

Before acquiring data with actual samples, we obtain system response curves using just the two injectors with no sample in between. This allows us to deconvolute the stray volume of the injection set-up out of the experimental data using a Laplace transform procedure described previously (Charlaix et al., 1986, 1987). The deconvoluted data are then fitted with theoretical models. In very homogeneous materials, the curves fit very well to a Gaussian dispersion.

When the dispersion is anomalous (i.e., experimental curves do not correspond to solutions of Eq. 1), we fit the data to the more complex capacitance model described in the literature (Coats and Smith, 1964; Schweich, 1985; Villermaux, 1981. This model assumes that only a fraction f of the fluid in the pore volume is actually flowing, with a corresponding dispersion coefficient K. Tracer exchange between the stagnant and flowing phases takes place with a characteristic time T_f. Dispersion in the flowing phase is characterized by a coefficient K. The fourth parameter is the mean intersticial velocity U.

The parameters in this model have no physical relationship to our sintered samples because the pore volume is well connected in our porosity range and no large dead zones can be viewed on micrographs. This procedure is however very convenient to compare data from various samples (f gives, for instance, the degree of deviation from a Gaussian behavior); it allows, in addition, a determination from these parameters of an asymptotic dispersion coefficient K_{as} with:

$$K_{as} = K + U^2 T_f (1 - f)^2 \tag{3}$$

K_{as} is the dispersion coefficient in a sample made of the same material but with a very large length compared to UT_f. One can indeed show that, in this case, the dispersion should become

Table 1. Data Obtained Using Bidisperse Sintered Samples Prepared from 320 and 95 μm Mean Dia. Glass Beads

Q mL/min	T_o s	Pe	V_{pa} cm^3	K_{as}/U cm	f	T_f s	ℓ_d/L_2
30% Porosity, 30% Small Beads Vol. Frac. Sample							
0.92	227	84.8	3.48	0.0143	0.98	NM*	0.751
0.46	458	42.1	3.51	0.0123	0.99	NM*	0.646
0.23	905	21.3	3.47	0.0118	0.98	NM*	0.622
0.092	2,285	8.42	3.50	0.0126	1	NM*	0.666
0.046	4,630	4.16	3.55	0.0143	1	NM*	0.754
0.023	9,320	2.07	3.57	0.0127	1	NM*	0.668
18% Porosity, 18% Small Beads Vol. Frac. Sample							
4.5	49.6	364	3.72	0.161	0.88	41.7	7.09
2.25	91.5	198	3.43	0.123	0.95	227	5.39
1.125	169	107.0	3.17	0.115	0.96	775	5.05
0.45	404.5	44.7	3.03	0.055	0.96	2,083	4.92
0.112	1,670	10.8	3.12	0.07	0.92	879	4.08
12% Porosity, 28% Small Beads Vol. Frac. Sample							
2.76	28.9	364	1.33	0.524	0.86	98.5	26.9
1.38	51.7	204	1.19	0.331	0.91	249	17.0
0.687	97.7	107.7	1.12	0.416	0.87	330	21.4
0.276	233	45.0	1.07	0.453	0.87	831	23.2
0.138	461	22.8	1.06	0.411	0.86	1,251	21.1
0.0687	899	11.7	1.03	0.377	0.86	2,157	19.3
0.0276	2,231	4.71	1.03	0.428	0.84	4,657	21.9
22% Porosity, 11% Small Beads Vol. Frac. Sample							
2.29	70.2	254	2.68	0.318	0.95	822	12.3
0.92	173	103	2.65	0.197	0.96	1,930	7.65
0.229	691	25.8	2.63	0.224	0.96	8,310	8.70
0.092	1,727	10.3	2.65	0.210	0.96	18,300	8.12
0.046	3,430	5.20	2.63	0.159	0.96	28,100	6.15
0.0229	6,790	2.63	2.60	0.107	0.96	36,600	4.69
0.0092	17,300	1.03	2.60	0.0858	0.96	62,000	3.33
Samples Obtained from Monodisperse Glass Beads							
34% Porosity Sintered 300 μm Dia. Beads							
1.125	154	102	2.89	0.00322	0.98	NM*	1.01
0.45	373	42.0	2.80	0.00424	0.98	NM*	1.33
0.225	905.5	17.4	3.40	0.00421	0.97	NM*	1.32
0.112	1,520	10.3	2.84	0.00399	0.96	NM*	1.25
0.045	3,760	4.17	2.82	0.00532	0.97	NM*	1.67

*NM: nonmeasurable.

Other data obtained with samples prepared from 200 μm dia. monodisperse glass beads are listed in Table 1 of Charlaix et al. (1987). Since, for these specimens, one has $L_2 = d$, the ratio ℓ_d/L_2 shown in the present paper is equivalent to the expression K_{as}/V_d in this previous reference.

Gaussian with a coefficient K_{as} provided that no correlations exist in the flow field at scales larger than the sample size. In the rest of this paper, we shall use K_{as} as the key parameter characterizing the magnitude of the dispersion effect.

Qualitative Analysis of Experimental Results

In Figure 1, we compare dispersion curves obtained with a monodisperse (Figure 1b) and a bidisperse (Figure 1a) sample with otherwise similar characteristics at a same flow rate of 0.276 mL/min. In order to make comparisons easier, the normalized conductivity variations are plotted vs. the ratio of the injected volume V to the total accessible porous volume V_{pa}. This plotting scheme will be kept throughout the paper, it allows us to eliminate the influence of the sample volume on the curves. V_{pa} is theoretically (Schweich, 1985; Villermaux, 1981) equal to the product QT_o where Q is the volume flow rate and T_o is the mean transit time. The monodisperse core is prepared from 200 μ dia. glass beads and has been very lightly sintered with a porosity of 34% (hardly 3% below the porosity of the nonconsolidated material). The second sample was obtained from a mixture of 320 and 95 μm beads. Its final porosity is 30% (Table 1), also only slightly below the porosity of the nonconsolidated material (individual beads can indeed be scratched away very easily). The characteristic length, defined in Eq. 10, is of the order of 180 μm, very close to that for the monodisperse sample. The volume fraction of small beads in the binary sample is close to the value corresponding to the porosity minimum well known in binary mixtures (Ben Aim and Legoff, 1967; Ben Aim, 1970). At this porosity minimum, we expected from previous results (Lemaitre, 1985; Lemaitre et al., 1986; Guennelon et al., 1983) a large dispersion (perhaps 100 times higher than for the monodisperse sample) and a very anomalous curve with a strong tailing effect. On the contrary, our dispersion curve for the binary sample, Figure 1a, is nearly Gaussian with almost no tail and a small dispersion coefficient (estimated from the large slope of the dispersion curve at the inflexion point). Both the tail and the dispersion amplitudes are on the order of or even lower than those corresponding to the monodisperse sample, Figure 1b.

How can this discrepancy be explained? First, it is extremely unlikely that the degree of sintering during the preparation can

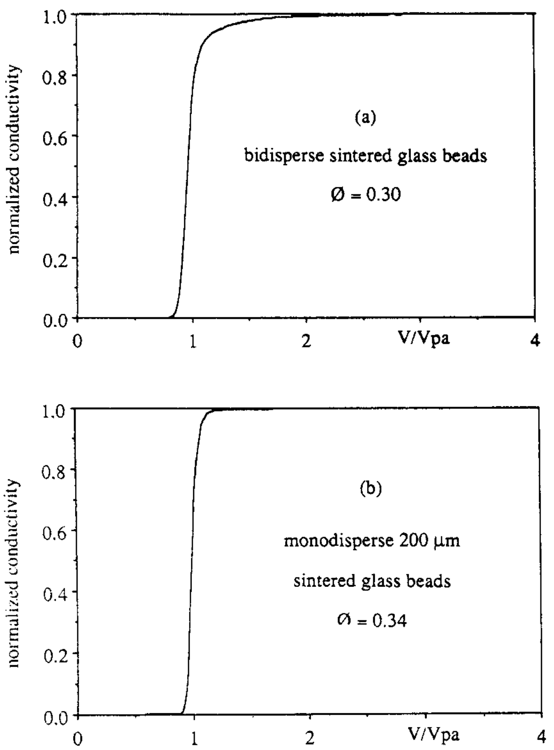

Figure 1. Normalized conductivity vs. V/V_{pa} for monodispersed and bidispersed samples.

modify so drastically the sample characteristics. The main difference is, in our opinion, that in the previous works (Lemaitre; Lemaitre et al.; Guennelon et al.) all the volume filled with powder is taken into account during the dispersion experiment, including the volume in the vicinity of the container walls. In the present experiment, the experimental sample is cored out of a much larger sintered glass cylinder. The influence of permeability variations across the sample cross section or near the walls is strongly reduced because we study a small part of the total sample. In the previous works, it has been seen that inhomogeneities introduced during the filling process strongly influence the dispersion characteristics. This hypothesis has been confirmed by recent CAT-scanner measurements (Gauthier, 1986) of the porosity distribution in similar nonconsolidated bidisperse mixtures inside columns with a diameter of several cm. Porosity variations of a few percent which are large enough to explain the large amount of dispersion in these systems have been observed across the section of these samples. It is very clear experimentally (Lemaitre; Lemaitre et al.) that these imperfections become much larger at mixture compositions corresponding to a porosity minimum. This in itself is a very interesting physical effect perhaps related to the flow properties of the mixtures. The influence of wall effects has also been shown during our dispersion measurements in monodisperse beads (Charlaix et al., 1986, 1987): the effective dispersion coefficient is significantly higher for samples coated with a low-viscosity epoxy penetrating the sample on a thickness of one or two mm than when a very viscous epoxy coating is used. A similar discrepancy, although much smaller, exists between our measurements and the increase of the dispersion coefficient by a factor of 2 also observed by Han et al. (1985) on unconsolidated mixtures with two peaks in the diameter distribution; these authors use a rather different size distribution from ours (small fraction of large spheres with a diameter on the average four times larger than that of small spheres). In this case, too, nonuniformities of the mixture may explain the dispersion coefficient differences; for instance, if clusters of large spheres buildup, they will induce significant permeability inhomogeneities.

At this point, using the above qualitative observations, there seems to be no intrinsic drastic effect of the polydispersity on tracer dispersion. Let us now investigate the evolution of the dispersion curves at constant flow rate values and mixture compositions when the degree of compaction of the material is increased. Figure 2 shows three dispersion curves at the same flow rate of 0.276 mL/min corresponding to three bidisperse samples of decreasing porosities obtained from similar bead mixtures. While dispersion in the lightly sintered sample (Ø = 30%) is low and almost Gaussian, Figure 2a, it increases markedly at Ø = 18%, Figure 2b, where a small tail appears. At Ø = 12%, dispersion is still higher and definitely non-Gaussian, Figure 2c. These results are qualitatively similar to those reported by Charlaix et al. (1986, 1987) for monodisperse samples of increasing compaction. Unfortunately it is not possible to obtain reference data for a nonconsolidated bidisperse material since this implies coring a sample out of a powder, a highly inconvenient and perturbative process.

Finally, a first view of the dependence of the dispersion coefficient on the Peclet number is obtained by superimposing normalized conductivity variations measured at six different flow rates ranging from 1.38 to 0.0276 mL/min for the same 12% porosity bidisperse sample, Figure 3. The horizontal axis, as

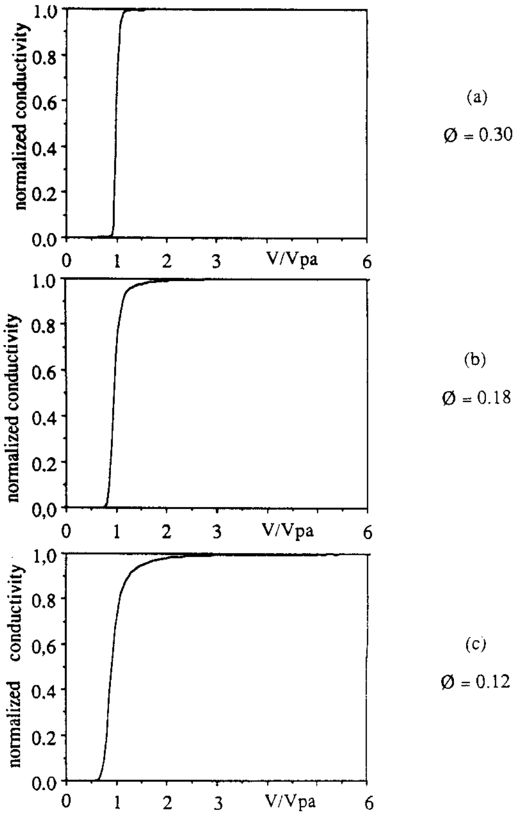

Figure 2. Normalized conductivity vs. V/V_{pa} for three bidispersed samples.

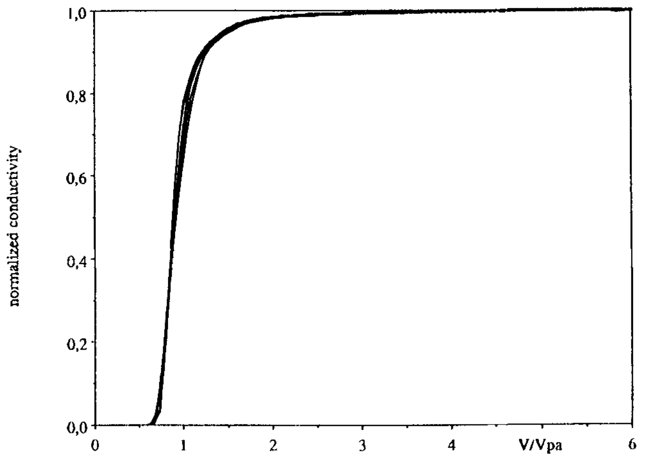

Figure 3. Normalized conductivity vs. V/V_{pa} at different flow velocities.

before, corresponds to the ratio of the injected fluid volume to the total pore volume; the vertical axis represents the normalized conductivity. In these axes, a dispersion coefficient K proportional to the Peclet number Pe gives a slope independent of Pe (if $K \propto Pe^2$, the step gets broader as Pe increases; in contrast if K = constant, the step gets steeper). We observe that all curves superimpose very well; this suggests a variation of K approximately proportional to Pe. This behavior, again, is very similar to those obtained for monodisperse samples. Thus, geometrical dispersion should be the dominant effect; again, no drastically new dispersion mechanism is introduced.

Quantitative Dispersion Parameter Variations

Let us now analyze results of the capacitance model applied to the dispersion curves obtained for the same three samples discussed above. A list of the values obtained from these fits for different monodisperse and bidisperse samples is given in Table 1.

We have first checked whether, at the end of the experiment, the tracer concentration reaches its new limit in the whole accessible porous volume V_{pa}. As said above, the product of the flow rate Q and the parameter T_o should, in that case, be equal to V_{pa} (Villermaux, 1981) and therefore should remain constant at all flow rates. We verified indeed that, for all three samples, the product T_oQ remains constant within ±5%. The precision is better for samples with the largest volumes for which the deconvolution computation is more accurate.

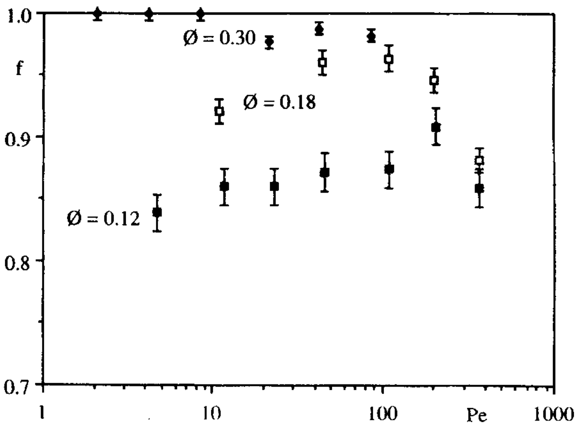

Figure 4. Flowing fraction vs. Peclet number.

Figure 4 shows the variation with Pe of the flowing fraction f for the same three samples as displayed in Figure 2. We shall only use the parameter f to characterize the magnitude of the deviation from a Gaussian behavior. The Peclet number $Pe = Ua/D_m$ is taken equal to:

$$Pe = \frac{\frac{L}{T_o} L_2}{D_m} \tag{4}$$

where D_m is the molecular diffusion coefficient, L is the total length of the sample, and L_2 is a characteristic microscopic length scale defined as the ratio of the total solid grain volume to the total grain area before sintering. L_2 is given by the formula:

$$L_2 = \frac{[ND_1^3 + (1 - N)\,D_2^3]}{[ND_1^2 + (1 - N)\,D_2^2]} \tag{5}$$

where N is the fraction in number of the spheres of diameter D_1 in the mixture, and D_1 and D_2 are the original individual diameters of the spheres in the nonconsolidated mixture. For the very lightly sintered sample (Ø = 30%), f is always above 0.98. At the lowest velocities, the curves are Gaussian within experimental uncertainty. When the degree of sintering increases, f goes down to 0.95 for Ø = 18% and to 0.85 for Ø = 12%. Although the corresponding curves display significant tails, these are smaller than in monodisperse samples with similar degrees of sintering (Charlaix et al., 1986, 1987). Once again, no large dispersion anomalies due to polydispersity are observed. As for monodisperse samples, f decreases at higher degrees of compaction.

Figure 5 displays for the same three samples as in Figure 4 the variations of the characteristic length $\ell_d = K_{as}/U$ with Peclet number. (Note that ℓ_d is obtained from the asymptotic dispersion coefficient defined in Eq. 3.) As stated previously, ℓ_d corresponds to the correlation length of the velocity field inside the sample and is the key information given by the dispersion measurement. Let us first notice the increase of ℓ_d by a factor of 30 between Ø = 30% and Ø = 12%; in the latter case, the correla-

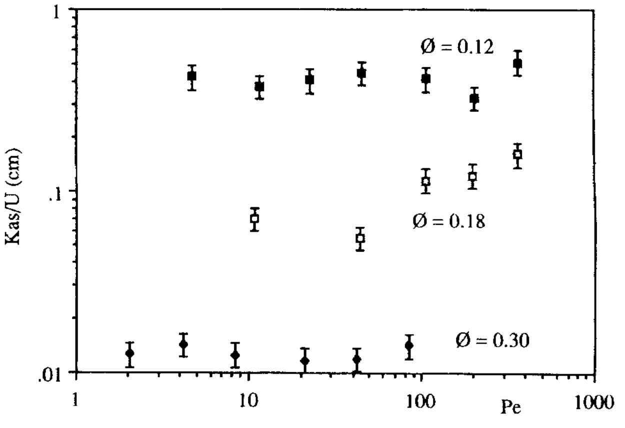

Figure 5. Variations of dispersion length vs. Peclet number.

tion length is up to about 6 mm. The sintering process increases very strongly the dispersion magnitude, just as for monodisperse sintered samples. The second important feature (already apparent from a qualitative analysis) is the weak variation of ℓ_d with the flow rate in the Peclet number range we have used. In that domain, geometrical dispersion is therefore dominant. Since ℓ_d is almost constant with *Pe*, from now on we shall compare dispersion in different samples by using the corresponding value of ℓ_d at some intermediate value of the Peclet number (typically around 50).

A major problem in the interpretation of dispersion experiments is making comparisons among data obtained on samples prepared from different sizes of beads, or from grains with a very broad size distribution.

Recently, conductivity and permeability measurements have been reported on the same sintered samples as used in the present work (Wong et al., 1984; Guyon et al., 1987). The variation of these parameters with the degree of sintering and the mixture composition is smooth and does not display any discontinuities. One obtains from these measurements a characteristic length scale

$$L_1 = F\sqrt{k} \tag{6}$$

where k is the permeability of the fluid and F is the ratio of the conductivity of a fluid to the conductivity of the porous media saturated with the fluid. In sintered materials made from monodisperse beads (Wong et al., 1984), L_1 is equal to the bead diameter. In bidisperse samples (Guyon et al., 1987), the experiments show that, at all degrees of sintering, L_1 is approximately equal to the length scale L_2 defined above by Eq. 5. The key feature of this characteristic length scale L_1 obtained from conductivity and permeability measurements is therefore that it does not depend on the degree of sintering (for porosities between 10 and 40%) and that it varies smoothly with the mixture composition.

A major objective of our work is to compare this result with the variation of the characteristic length ℓ_d obtained from dispersion measurements on similar samples. For that purpose we have chosen to characterize the magnitude of the tracer dispersion by a dispersion ratio:

$$R = \frac{\ell_d}{L_1} \simeq \frac{\ell_d}{L_2} \tag{7}$$

This novel approach is preferable to the use of the correlation length ℓ_d of the velocity only; dividing ℓ_d by L_2 or L_1 eliminates indeed the influence the mean size of the nonconsolidated mixture. In this way, characteristics of porous media from very diverse origins can be compared.

In Figure 6 we plot the variation of R against the difference $\triangle\varnothing$ of the sample porosity $\varnothing$ and of the porosity $\varnothing_{nc}$ for a nonconsolidated sample of the same composition. $\varnothing_{nc}$ has been estimated from the work of Ben Aim and Legoff (1967), Ben Aim (1970) Lemaitre (1985) and Lemaitre et al. (1986). In this way variations of the porosity $\varnothing$ directly associated to the polydispersity are eliminated. In Figure 6 the open squares correspond to data for four monodisperse samples prepared from 200 μm dia. beads with respective porosities of 37 (nonconsolidated sample), 34, 24, and 14%. These samples are those studied previously (Charlaix et al., 1987). The solid line represents a best fit to these four data points. The black diamonds correspond to data for the three bidisperse samples with porosity equal to 30, 18, and 12%. These data are the same as used in Figures 2, 4, and 5. We also include data for one bidisperse sample (black square) prepared from glass beads of 320 and 95 μm mean dia. with an 11% volume fraction of small beads with a sample porosity of 22%. Finally, we show data for one monodisperse sample (open diamond) prepared from 320 μm mean dia. beads with a 33% porosity. The length ℓ_d values have been determined at fluid velocities in the intermediate Peclet number range (typically between 20 and 100).

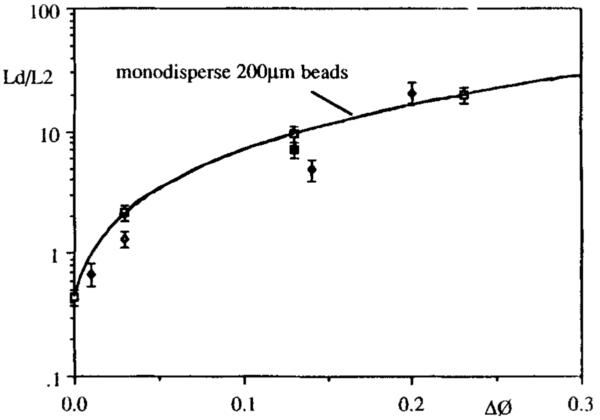

Figure 6. *R* vs. $\Delta\phi$.

For the nonconsolidated monodisperse sample ($\triangle\varnothing = 0$), R is of the order of 0.5; in this case, there are no large-scale inhomogeneities, and the velocity correlation length is about the grain size. This R value represents a lower limit. If the flow is not turbulent, the correlation range of the velocity field will be at least equal to an individual pore size. For the least consolidated bidisperse sample ($\triangle\varnothing = 0.015$), R is about 0.7 and similar to the monodisperse results. Therefore we can deduce that the mixture is homogeneous above a scale of no more than two or three grain sizes.

At higher degrees of sintering ($\triangle\varnothing = 0.13$ and $\triangle\varnothing = 0.19$), the variation of R is similar for the bidisperse samples studied above and the monodisperse samples. In both cases, R is 50 times higher for $\triangle\varnothing = 0.2$–$0.25$ than for a nonconsolidated sample ($\triangle\varnothing = 0$). ℓ_d is very sensitive to inhomogeneities introduced by the sintering process while L_1 and L_2 remain constant. Experimental points for the other samples, corresponding to different volume fractions of small beads, follow the general trend of variation with $\triangle\varnothing$. The deviations are probably associated with the sensitivity of the technique to slight variations in the packing or sintering procedure.

Conclusions

A first key result of this work is that it is possible to characterize the heterogeneity of a sintered material by a parameter R independent of the initial mixture composition and grain size. R is equal to the ratio of the length scale $\ell_d = K_{as}/V$ obtained from the dispersion measurements by the scale L_1 defined by Wong et al. and Guyon et al. from conductivity and permeability values. This dispersion ratio is an original characterization of the scale of the heterogeneities of the flow and of the mixing efficiency of the porous medium. Our measurements on both monodisperse and bidisperse samples show indeed that R depends mostly on the degree of sintering (for a given sintering and filling procedure) and not on the characteristics of the mixture. The same large R variations with the degree of sintering (factors of 30 or 60) are obtained in both monodisperse and bidisperse samples.

A second important result is that lightly sintered bidisperse samples display a regular Gaussian dispersion behavior, even at mixture compositions close to the porosity minimum. This latter result is in contrast with the huge dispersion anomalies reported by Guennelon et al., Lemaitre, and Lemaitre et al. in nonconsolidated binary mixtures with similar compositions. We believe that these effects are associated with permeability inhomogeneities across the sample cross section, particularly at the container walls. We do not observe these effects because we core out a small part of the total sample (located near the center) to perform our experiments. In addition, the improved filling process we use probably further reduces the amount of heterogeneities.

In short, the present results confirm that tracer dispersion is a measurement mostly sensitive to large-scale heterogeneities and long-range fluid velocity correlations rather than to microscopic details. A next step is to examine why sintering processes may introduce such large-scale inhomogeneities. A possible approach is to improve the filling and sintering techniques and determine whether the final amount of dispersion can be reduced. Other experimental techniques sensitive to nonlocal effects will have to be used in order to cross-correlate the results with the dispersion measurements. It is an open problem on which active work is being done in our laboratory. We seek to correlate quantitatively the value of ℓ_d to the extremely heterogeneous nature of random cuts of pore space obtained for heavy sintering (contrasting with the regular one obtained for light sintering). Image analysis and mercury porosimetry are two possible candidates. In the latter technique, the invasion of a pore by mercury at a given injection pressure is determined by the presence of a continuous chain of large pores connecting it to the injection point. Another need is to correlate quantitatively dispersion anomalies to heterogeneity sizes or permeability contrasts. Information on this problem will be obtained using, for instance, artificially prepared layered samples.

Finally, all these problems encountered in sintered materials are closely related to those found in real rocks. The study of heterogeneities introduced during the sintering will indeed give crucial information on those introduced in rocks by the diagenesis process. A proper analysis of the influence of the sintering and filling processes on the dispersion characteristics will be an important step toward this goal.

Acknowledgment

We wish to thank J. Koplik, J. Lemaitre, and D. Wilkinson for many helpful discussions, and J. Bubori, P. Gerardi, M. Ridge, and D. Rossini for their technical assistance. We also thank the Schlumberger EPS Clamart center for the use of their computing facilities.

Notation

a = characteristic microscopic length of flow channels in a porous medium
D_1, D_2 = diameter of individual spheres
D_m = molecular diffusion coefficient
f = flowing fraction, Eqs. 4, 5
F = formation factor
k = permeability
$K_\parallel$ = dispersion coefficient parallel to flow
$K_\perp$ = dispersion coefficient perpendicular to flow
K_g = dispersion coefficient value obtained from a best fit with a Gaussian model
K = dispersion coefficient from four-parameter model
K_{as} = asymptotic dispersion coefficient
ℓ_d = characteristic length scale obtained from dispersion measurement, Eq. 2
L = sample length
L_1 = characteristic microscopic length scale obtained from resistivity and permeability measurements, Eq. 16
L_2 = characteristic microscopic length scale defined from volume-to-surface ratio, Eq. 15
N = fraction in number of sphere with a diameter D_1
Pe = Peclet number, Eq. 4
Q = liquid flow rate
T_f = characteristic exchange time between the stationary and flowing fluids from four-parameter model
T_o = mean transit time through sample
$u_\parallel$ = local velocity component parallel to flow
U = mean interstitial flow velocity
V_{pa} = accessible porous volume computed from product QT_o
$\varnothing$ = sample porosity
$\varnothing_{nc}$ = porosity of nonconsolidated sample prepared from same bead mixture
$\triangle\varnothing = \varnothing - \varnothing_{nc}$

Literature Cited

Bacri, J. C., N. Rakotomalala, and D. Salin, "Experimental Evidence of Disorder Effects in Hydrodynamic Dispersion," *Phys. Rev. Lett.*, **58,** 2035 (1986).

———, "Stable and Unstable Miscible flows through Porous Media," *AIP Conf. Proc.*, **154:** *Physics and Chemistry of Porous Media II,* AIP, New York (1987).

Baker, L. E., "Effects of Dispersion and Dead End Pore Volume in Miscible Flooding," *Soc. Pet. Eng. J., Trans. AIME,* **263,** 219 (1975).

Bear, J., *Dynamics of Fluids in Porous Media,* Elsevier, New York, ch. 10 (1972).

Ben Aim, R., "Etude de la Texture des Empilements de Grains, Application à la Détermination de la Perméabilité des Mélanges Binaires en Régime Moléculaire, Intermédiaire, Laminaire," Thèse de Doctorat d'Etat, Nancy (1970).

Ben Aim, R., and P. Legoff, "Effets de Parois dans les Empilements Désordonnés de Sphères et Application à la Porosité des Mélanges Binaires," *Powder Technol.,* **1,** 281 (1967).

Charlaix, E., J. P. Hulin, and T. J. Plona, "Etude Experimentale de la Dispersion d'un Traceur dans des Echantillons de Billes de Verre Frittees," *C.R. Acad. Sc. Paris,* **303,** II, 1413 (1986).

———, "Experimental Study of Tracer Dispersion in Sintered Glass Materials of Variable compaction," *Phys. Fluids,* **30,** 1690 (1987).

Coats, K. H., and B. D. Smith, "Dead End Pore Volume and Dispersion in Porous Media," *Soc. Pet. Eng. J., Trans. AIME,* **231,** 73 (1964).

Fried, J. J., and M. A. Combarnous, "Dispersion in Porous Media," *Adv. Hydrosci,* **7,** 169 (1971).

Gauthier, J., "Sur les Distributions de Temps de Séforu d'un Fluide dan des Empilements de Billes de Verre de Deux Tailles," submitted to *C. R. Acad. Sc. Paris* (1987).

Guennelon, R., A. Zeiliguer, and A. M. de Cockborne, "Effets Texturaux sur la Porosite et la Dispersion Hydrodynamique," *Proc Colloq. "Variabilité Spatiale des Processus de Transfert dans les Sols," Avignon, 24-25 Juin 1982, Colloques de l'INRA,* **15,** 133 (1983).

Guyon, E., L. Oger, and T. J. Plona, "Transport Properties in Sintered Porous Media Composed of Two Particle Sizes," *J. Phys. D.,* **20,** 1637 (1987a).

Guyon, E., Y. Pomeau, J. P. Hulin, and C. Baudet, "Dispersion in the Presence of Recirculation Zones," *Nuc. Phys. B (Proc. Suppl.),* **2,** 271 (1987).

Han, N. W., J. Bhakta, and R. G. Carbonell, "Longitudinal and Lateral Dispersion in Packed Beds: Effect of Column Length and Particle Size Distribution," *AIChE J.,* **31,** 277 (1985).

Hulin, J. P., and D. Salin, "Experimental Study of Tracer Dispersion in Model and Natural Porous Media," *Proc. Cargese NATO School on Mixing and Disorder,* E. Guyon, J. P. Nadal, Y. Pomeau, eds., Nijhoff (1987).

Koch, D. L., and J. F. Brady, "Dispersion in Fixed Beds," *J. Fluid Mech.,* **154,** 399 (1985).

———, "Nonlocal Dispersion in Porous Media: Nonmechanical Effects," submitted to *Chem. Eng. Sci.* (1987).

Lemaitre, J., "Propriétés de Transport dans l'Espace des Pores d'un

Empilement: Influence de la Dispersion de Taille des Cavités," Thèse, Université de Rennes (1985).

Lemaitre, J., M. Cintre, J. P. Troadec, and D. Bideau, "Dispersion d'un Traceur dans un Mélange Binaire de Sphères," *C.R. Acad. Sci. Paris* (1986).

Redner, S., "Dynamical Processes in Random Media, in *Proc. de l'Ecole d'Hiver des Houches on Physics of Finely Divided Matter,* M. Daoud, N. Boccara, eds. Springer, 113 (1985).

Saffman, P. G., "A Theory of Dispersion in Porous Media," *J. Fluid Mech.,* **6,** 321 (1959).

———, "Dispersion Due to Molecular Diffusion and Macroscopic Mixing in Flow through a Network of Capillaries," *J. Fluid Mech.,* **7,** 194 (1960).

Schweich, D., "Flow in Porous Media and Residence Time Distribution," *Proc. de l'Ecole d'Hiver des Houches on Physics of Finely Divided Matter,* M. Daoud, N. Boccara, eds. Springer, 329 (1985).

Taylor, G. I., "Dispersion of Soluble Matter in Solvent Flowing Slowly through a Tube," *Proc. Roy. Soc. A,* **219,** 186 (1953).

———, "Conditions under which Dispersion of a Solute in a Stream of Solvent Can be Used to Measure Molecular Diffusion," *Proc. Roy. Soc. A,* **225,** 473 (1954).

Villermaux, J., "Theory of Linear Chromatography," *Percolation Processes, Theory and Applications," NATO Adv. Studies Inst.* **E33,** Sijtoff and NoordHoff, eds. (1981).

Wong, P. Z., J. Koplik, and J. Tomanic, "Conductivity and Permeability of Rocks," *Phys. Rev. B,* **30,** 6606 (1984).

Manuscript received Mar. 18, 1987, and revision received Dec. 8, 1987.